



ELSEVIER

Available online at [www.sciencedirect.com](http://www.sciencedirect.com)

ScienceDirect

<http://www.elsevier.com/locate/biombioe>

# The influence of feedstock and production temperature on biochar carbon chemistry: A solid-state $^{13}\text{C}$ NMR study

Anna V. McBeath<sup>a,\*</sup>, Ronald J. Smernik<sup>a</sup>, Evelyn S. Krull<sup>b</sup>, Johannes Lehmann<sup>c</sup>

<sup>a</sup> School of Agriculture Food and Wine and Waite Research Institute, The University of Adelaide, Waite Campus, PMB 1, Glen Osmond, SA 5064, Australia

<sup>b</sup> CSIRO Land and Water, PMB 2, Glen Osmond, SA 5064, Australia

<sup>c</sup> Department of Crop and Soil Sciences, Cornell University, Ithaca, NY 14853, United States

## ARTICLE INFO

### Article history:

Received 22 May 2013

Received in revised form

3 October 2013

Accepted 7 November 2013

Available online 26 November 2013

### Keywords:

Biochar

Solid-state  $^{13}\text{C}$  NMR spectroscopy

Aromatic condensation

Mean residence time

Carbon sequestration

Pyrolysis

## ABSTRACT

Solid-state  $^{13}\text{C}$  nuclear magnetic resonance (NMR) spectroscopy was used to evaluate the carbon chemistry of twenty-six biochars produced from eleven different feedstocks at production temperatures ranging from 350 °C to 600 °C. Carbon-13 NMR spectra were acquired using both cross-polarisation (CP) and direct polarisation (DP) techniques. Overall, the corresponding CP and DP spectra were similar, although aromaticity was slightly higher and observability much higher when DP was used. The relative size and purity of the aromatic ring structures (i.e. aromatic condensation) were also gauged using the ring current technique. Both aromaticity and aromatic condensation increased with increasing production temperature, regardless of the feedstock source. However, there were clear differences in these two measures for biochars produced at the same temperature but from different feedstocks. Based on a relationship previously established in a long-term incubation study between aromatic condensation and the mean residence time (MRT) of biochar, the MRT of the biochars was estimated to range from <260 years to >1400 years. This study demonstrates how the combination of feedstock composition and production temperature influences the composition of aromatic domains in biochars, which in turn is likely to be related to their recalcitrance and ultimately their carbon sequestration value.

© 2013 Elsevier Ltd. All rights reserved.

## 1. Introduction

The term biochar refers to carbon-rich materials purposely produced for addition to soils through the process of pyrolysis of waste organic feedstock [1]. Over the past decade, there has

been much interest in biochar as a sustainable means to sequester atmospheric carbon, improve soil fertility, reduce greenhouse gas emissions and improve waste management [1,2]. The carbon sequestration potential of biochar can be attributed to its recalcitrant nature and hence long turnover time in soils. However, several studies have questioned this

\* Corresponding author. School of Earth and Environmental Sciences, James Cook University, PO Box 6811, Cairns, Queensland 4870, Australia. Tel.: +61 07 4042 1696.

E-mail addresses: [anna.mcbeath@jcu.edu.au](mailto:anna.mcbeath@jcu.edu.au) (A.V. McBeath), [ronald.smernik@adelaide.edu.au](mailto:ronald.smernik@adelaide.edu.au) (R.J. Smernik), [CL273@cornell.edu](mailto:CL273@cornell.edu) (J. Lehmann).

0961-9534/\$ – see front matter © 2013 Elsevier Ltd. All rights reserved.

<http://dx.doi.org/10.1016/j.biombioe.2013.11.002>

longevity by providing examples where turnover times in soil are relatively short (<50 years) [3–5]. Therefore, in order for biochar to be used as a carbon sequestration tool as part of a global carbon trading scheme, reliable and cost-effective methods need to be developed that can predict and verify the stability of a range of biochars that vary in feedstock and types of production. Mean residence times (MRT) of individual biochars can be determined from long-term incubation experiments [6–8]. However, given that such data requires months to years to obtain, a more practical solution is required. Recently, we reported strong relationships between MRT values determined in long-term incubation experiments and measures of aromaticity and aromatic condensation determined by NMR spectroscopy [9].

Biochar is not a unique material in the chemical sense, but rather a range of materials that differ as a consequence of several factors including feedstock composition, highest heating temperature and pyrolysis duration. As a consequence, the chemical composition and physical structure of different biochars are also expected to vary considerably in terms of their organic and ash content, pH, particle size, porosity, surface area and many other properties. However, all biochars are to a greater or lesser degree composed of condensed aromatic ring structures. These structures become larger and more condensed with increasing production temperature [10].

Variability among biochars can have a significant effect on their role and fate in soils, and, most importantly, has been reported to influence their chemical stability in soils [11]. Hamer et al. [12] observed that maize and rye biochars were mineralised more rapidly than wood biochar. This difference was attributed to wood biochar having a greater aromatic C content. Nguyen and Lehman [13] reported effects of both feedstock and production temperature of biochar on its mineralisation. They found that mineralisation significantly decreased at higher production temperatures for corn biochars but found no change in mineralisation rates for oak biochars [13]. Similarly, Baldock and Smernik [14] reported that the rate of biochar mineralisation decreased with increasing production temperature for pine biochar. This was attributed to biochars produced at lower temperatures containing less aromatic C. Singh et al. [9] also found that both production temperature and feedstock affected the mineralisation rate of biochar, with biochars produced at 400 °C mineralised more rapidly than those produced at 550 °C and wood-derived biochars mineralised more slowly than those produced from feedstocks such as manures and paper mill waste.

The effects of feedstock and production temperature on biochar properties can be quite complex. Ascough et al. [15] reported that as biochars reach production temperatures of 600 °C, their structures become increasingly similar and independent of the feedstock, as determined using solid-state <sup>13</sup>C NMR spectroscopy. This is consistent with a model of char evolution developed by Keiluweit et al. [16] in which differences in the chemical composition of chars produced from different feedstocks are lost during an early transition stage but differences in physical structure remain through later stages. It is also consistent with our recent finding of two distinct phases in charcoal formation: first an increase in

aromaticity, followed by a structural rearrangement creating condensed aromatic structures [17].

The development of analytical techniques sensitive to differences in the chemical composition of biochar is not only important for predicting biochar properties (and especially resistance to decomposition) but would also enable better interpretation of existing published data. Our current knowledge of biochar fate and behaviour is based on experiments involving many different biochars produced across a wide range of production temperatures and from a variety of feedstocks. Until now it has been very difficult to compare findings across such studies and interpret how differences in biochar composition may have influenced results.

In this study, we investigate a set of biochars produced from various feedstocks at a range of production temperatures and under differing pyrolysis conditions. Two different solid-state <sup>13</sup>C NMR spectroscopic techniques are used in order to measure the aromaticity and the aromatic condensation of the biochars, two properties proven to be correlated with biochar mineralisation rate in long-term (5-year) incubation experiments [9]. The main aim is to investigate how feedstock and pyrolysis conditions influence these properties in combination with production temperature, furthering our earlier investigations that focussed solely on the effect of production temperature for biochars produced from a single woody feedstock [17].

---

## 2. Materials and methods

### 2.1. Biochar feedstocks and production conditions

Twenty-six biochar samples were investigated in this study, produced using three different pyrolysis processes. Production of twenty-one of these biochars (bull, dairy, hazelnut, oak, pine, food, paper) has been described elsewhere [18]. Briefly, these biochars were produced using a slow pyrolysis process by Best Energies Inc. (Cashton, WI, USA) using the Daisy Reactor and the following feedstocks: bull manure with sawdust (Bull Manure), corn stover (Corn), dairy manure with rice hulls (Dairy Manure), hazelnut shells (Hazelnut), oak wood (Oak), pine wood (Pine), food waste (Food) and white paper mill sludge (Paper). Soybean and switch grass biochars were produced using a fast pyrolysis reactor at 500 °C as described in Ref. [19]. The bamboo biochars were produced using a slow pyrolysis reactor by Hangzhou Sustainable Food and Fuel Enterprise, China; no further production details were available, except for the production temperature. Further details, including feedstock source, target temperature, ramp time and holding time, of all biochars are detailed in [Results and Discussion, Table 1](#).

### 2.2. Carbon content

Biochar samples were air-dried and finely powdered using a pestle and mortar. Total C content was determined in duplicate using a LECO CNS2000 carbon analyser (LECO Corporation, St Joseph, MI). An uncertainty of ±2% is estimated based on these duplicate measurements.

**Table 1 – Properties of biochars.**

| Sample ID            | Feedstock                    | Target temperature (°C) | Ramp time (min) | Hold time (min) | C content (g/kg) | Fe (mg/kg) |
|----------------------|------------------------------|-------------------------|-----------------|-----------------|------------------|------------|
| <i>Wood</i>          |                              |                         |                 |                 |                  |            |
| Oak 350              | Oak wood                     | 350                     | 80–90           | 15–20           | 713              | 496        |
| Oak 450              | Oak wood                     | 450                     | 80–90           | 15–20           | 820              | 47.5       |
| Pine 450             | Pine wood                    | 450                     | 80–90           | 15–20           | 791              | 65.6       |
| Pine 550             | Pine wood                    | 550                     | 80–90           | 15–20           | 853              | 25.6       |
| <i>Crop residues</i> |                              |                         |                 |                 |                  |            |
| Hazelnut 350         | Hazelnut shells              | 350                     | 80–90           | 15–20           | 722              | 84.9       |
| Hazelnut 450         | Hazelnut shells              | 450                     | 80–90           | 15–20           | 766              | 59.6       |
| Hazelnut 550         | Hazelnut shells              | 550                     | 80–90           | 15–20           | 838              | 97.9       |
| Corn 400             | Corn stalks                  | 400                     | 80–90           | 15–20           | 645              | 1340       |
| Corn 500             | Corn stalks                  | 500                     | 80–90           | 15–20           | 661              | 1960       |
| Corn 600             | Corn stalks                  | 600                     | 80–90           | 15–20           | 678              | 2750       |
| Soy 500              | Soybean                      | 500                     | 30              | 30              | 602              | 1870       |
| Switch 500           | Switch grass                 | 500                     | 30              | 30              | 602              | 1320       |
| Bamboo 400           | Bamboo                       | 400                     | na              | na              | 681              | 31,000     |
| Bamboo 500           | Bamboo                       | 500                     | na              | na              | 702              | 8000       |
| Bamboo 600           | Bamboo                       | 600                     | na              | na              | 743              | 8050       |
| <i>Manures</i>       |                              |                         |                 |                 |                  |            |
| Bull manure 400      | Bull manure with sawdust     | 400                     | 80–90           | 15–20           | 686              | 252        |
| Bull manure 500      | Bull manure with sawdust     | 500                     | 80–90           | 15–20           | 728              | 547        |
| Bull manure 600      | Bull manure with sawdust     | 600                     | 80–90           | 15–20           | 742              | 337        |
| Dairy manure 400     | Dairy manure with rice hulls | 400                     | 80–90           | 15–20           | 659              | 407        |
| Dairy manure 600     | Dairy manure with rice hulls | 600                     | 80–90           | 15–20           | 732              | 427        |
| <i>Organic waste</i> |                              |                         |                 |                 |                  |            |
| Food 400             | Food waste                   | 400                     | 80–90           | 15–20           | 480              | 9120       |
| Food 500             | Food waste                   | 500                     | 80–90           | 15–20           | 538              | 4742       |
| Food 600             | Food waste                   | 600                     | 80–90           | 15–20           | 284              | 8790       |
| <i>Mill waste</i>    |                              |                         |                 |                 |                  |            |
| Paper 400            | Paper mill waste             | 400                     | 80–90           | 15–20           | 206              | 4216       |
| Paper 500            | Paper mill waste             | 500                     | 80–90           | 15–20           | 193              | 4485       |
| Paper 600            | Paper mill waste             | 600                     | 80–90           | 15–20           | 185              | 4345       |

### 2.3. Iron content

The total iron concentration of the biochars was determined using the method of Farrell et al. [20]. In brief, biochars were digested with a perchloric/nitric acid mixture in open digestion tubes in a heated block. Samples were filtered to 0.45  $\mu\text{m}$  and analysed by ICP-MS (7500cx, Agilent Technologies, CA, USA).

### 2.4. Solid-state $^{13}\text{C}$ NMR spectroscopy

Solid-state  $^{13}\text{C}$  magic angle spinning (MAS) NMR spectra were obtained at a frequency of 100.6 MHz on a Varian Unity INOVA 400 NMR spectrometer. Samples ( $\sim 200$  mg) were packed in 7-mm diameter cylindrical zirconia rotors with Kel-F rotor end-caps and spun at the “magic angle” ( $54.7^\circ$ ) at  $6500 \pm 100$  Hz in a Doty Scientific supersonic MAS probe. Free induction decays (FIDs) were acquired with a sweep width of 50 kHz; 1216 data points were collected over an acquisition time of 12 ms. All spectra were zero-filled to 8192 data points and processed with a 50-Hz Lorentzian line broadening and a 0.010-s Gaussian broadening. Chemical shifts were externally referenced to the methyl resonance of hexamethylbenzene at 17.36 ppm. Cross-polarisation (CP) spectra represent the accumulation of 4000 scans and were acquired using a  $90^\circ$   $^1\text{H}$  pulse of 5–6  $\mu\text{s}$  duration, a 1-ms contact time and a 1-s recycle delay. Direct polarisation (DP) spectra represent the

accumulation of 500–1000 scans and were acquired using a  $90^\circ$   $^{13}\text{C}$  pulse of 5–10  $\mu\text{s}$  duration and a 90-s recycle delay. Spin counting was carried out using the method of Smernik and Oades [21,22]. Glycine (AR grade, Ajax Chemicals) was used as the external reference for spin counting, i.e. the glycine spectrum was acquired separately to those of the samples. The percentage of total signal due to non-aromatic signal in the 10–50 ppm chemical shift range was determined by integration of both CP and DP spectra and subtracted from 100% to provide aromaticity as described in the Results section.

Aromatic condensation of biochars was measured using the method of McBeath and Smernik [23]. This technique utilises the upfield shift in the peak position of a probe molecule ( $^{13}\text{C}$ -benzene) that occurs when it is sorbed to a solid such as biochar that contains aromatic structures capable of sustaining ring currents. We denote this shift as  $\Delta\delta$  ( $\Delta\delta = \delta_{\text{sorbed benzene}} - \delta_{\text{neat benzene}}$ ). Previous replicate analyses have established uncertainty to be  $< \pm 0.4$  ppm [23]. For larger and more condensed aromatic structures,  $\Delta\delta$  becomes increasingly negative as the ring currents increase in strength. Aliquots of each biochar sample (200 mg) were placed in 2 mL glass vials with PTFE-lined screw caps. Neat  $^{13}\text{C}$ -labelled benzene (ca. 10  $\mu\text{l}$ ) from Cambridge Isotope Laboratories, Inc. (Andover, Massachusetts), was added using a micropipette and the samples were shaken for 1 min and stored at room temperature until analysed. Samples were analysed using



solid-state  $^{13}\text{C}$  CP NMR spectroscopy. Spectra were acquired using the same acquisition conditions described above but since far fewer scans (16–128) were required, acquisition times were very short (<5 min).

### 3. Results

Solid-state  $^{13}\text{C}$  CP and DP NMR spectra of the twenty-six biochars are shown in Fig. 1a–c. Nearly all of the spectra are dominated by the aromatic peak centred at around 130 ppm, which becomes increasingly dominant with increasing temperature. The predominance of aromatic C is consistent with numerous previously reported  $^{13}\text{C}$  NMR spectra of biochars [11,14,15,17,24–27]. The spectra also contain prominent spinning sidebands (SSBs) associated with the aromatic peak (marked with an asterisk in Fig. 1a–c). First order SSBs appear at around 65 ppm and 205 ppm, while smaller second order SSBs appear at around 0 ppm and 260 ppm. A third order SSB is visible at around –65 ppm for the bamboo 400 °C biochar. These spectral artifacts occur when the rate of magic angle spinning (MAS) is less than the chemical shift anisotropy (CSA) for a given resonance and could not be avoided due to practical limitations with our spectrometer set-up (400 MHz spectrometer with 7 mm rotors that have a maximum spinning speed of 6.5 kHz). The presence of these prominent SSBs compromised the quantification of the aromaticity of the biochars (see below).

Besides the aromatic peak at 130 ppm and its associated SSBs, the next most common signals appear in the alkyl region, with most spectra containing two broad signals at around 15 ppm and 35 ppm. The former can be identified as due to methyl ( $\text{CH}_3$ ) and the latter mostly due to methylene ( $\text{CH}_2$ ) carbon. The broadness of these peaks and their similar sizes suggests the majority of alkyl C is present in short side-chains attached to, or bridges between, aromatic structures [24,28]. The alkyl signal for the food 400 °C biochar (Fig. 1c) is exceptional in that it is larger, sharper and dominated by the  $\text{CH}_2$  resonance, indicating the presence of considerable long-chain alkyl groups.

Two of the lower temperature biochars, paper 400 °C and oak 350 °C (Fig. 1a and c), contain several clear and sharp peaks in the 55–110 ppm range, which can be attributed to carbohydrates. Similar spectra have been reported at the low temperature end of charcoal thermosequences [11,14,15,17,23,25,27,29] and indicate the presence of thermally untransformed or incompletely transformed biomass. The  $^{13}\text{C}$  DP NMR spectra of the paper biochars (Fig. 1c) produced at all three temperatures

(400 °C, 500 °C and 600 °C) each contain a sharp peak at 169 ppm. This peak is not detected in the corresponding CP spectra and can be attributed to carbonate [30]. The absence of this peak from the CP spectra can be attributed to the lack of  $^1\text{H}$  nuclei close to the  $^{13}\text{C}$  nuclei in carbonate minerals, which are required for cross-polarisation to occur. Previous analyses of these biochars have shown them to have high carbonate contents [18].

There are some other differences between corresponding CP and DP spectra. The broad alkyl signals at around 15 ppm and 35 ppm as well as the carbohydrate signal (in the 55–110 ppm range) tend to be larger in the CP spectra. This indicates that alkyl and carbohydrate C are detected with greater efficiency than aromatic C by CP [17].

While comparisons of the relative strength of signals between CP and DP spectra provide information about the relative detection efficiency of the two techniques for various C types, the overall detection efficiency is best determined by spin counting [21,22]. The observability of C ( $C_{\text{obs}}$ ) in the biochars, determined in this way, is shown in Table 2. Generally, observability for the DP spectra ( $C_{\text{obs-DP}} > 49\%$ ) was higher than for the CP spectra ( $C_{\text{obs-CP}} < 61\%$ ). This can be partly attributed to the low  $^1\text{H}$  content of the condensed aromatic units that form the bulk of the biochars' molecular structure. This low concentration of  $^1\text{H}$  nuclei reduces the efficiency of magnetisation transfer (cross-polarisation), especially for  $^{13}\text{C}$  nuclei more than three bonds removed from nearest  $^1\text{H}$  neighbours (remotely protonated  $^{13}\text{C}$  nuclei). Furthermore, high free radical content, especially for biochars produced in the 400–600 °C range where free radical content is maximised [31], also interferes with CP observability of biochars [11,29,32,33]. Paramagnetic and ferromagnetic minerals, especially iron minerals, can also affect NMR observability of charred materials [34]. The iron content (Table 2) was highest for the biochars produced from bamboo (8–31 g/kg) and food (4.7–9.1 g/kg) and this likely to have contributed to the very low CP observability for the bamboo 600 °C ( $C_{\text{obs-CP}} = 8\%$ ) and the food 600 °C biochars ( $C_{\text{obs-CP}} = 5\%$ ). The very low observability for these biochars explains why their CP spectra are very poor in terms of signal-to-noise ratio (Fig. 1b and c).

A key measure of biochar composition is its aromaticity, i.e. the proportion of the carbon in the material that is aromatic. However, quantification of aromaticity from the  $^{13}\text{C}$  NMR spectra of these biochars is compromised by two main factors: (i) the presence of the large SSBs that overlap with non-aromatic signal; and (ii) the low CP observability for all of the biochars and the low DP observability for a minority of the biochars. In addition, the aromatic peak and its SSBs are relatively broad making overlap between aromatic and non-

**Fig. 1** – a. Solid-state  $^{13}\text{C}$  CP and DP NMR spectra of biochars produced from wood feedstocks at production temperatures between 350 °C and 550 °C (Table 1). Asterisks (\*) mark the position of spinning sidebands (SSBs) associated with the aromatic peak at 130 ppm. Note that the high-field SSB (ca. 65 ppm) may overlap with O-alkyl signal at the same chemical shift. b. Solid-state  $^{13}\text{C}$  CP and DP NMR spectra of biochars produced from crop residue feedstocks at production temperatures between 400 °C and 600 °C (Table 1). Asterisks (\*) mark the position of spinning sidebands (SSBs) associated with the aromatic peak at 130 ppm. Note that the high-field SSB (ca. 65 ppm) may overlap with O-alkyl signal at the same chemical shift. c. Solid-state  $^{13}\text{C}$  CP and DP NMR spectra of biochars produced from organic waste and mill waste feedstocks at production temperatures between 400 °C and 600 °C (Table 1). Asterisks (\*) mark the position of spinning sidebands (SSBs) associated with the aromatic peak at 130 ppm. Note that the high-field SSB (ca. 65 ppm) may overlap with O-alkyl signal at the same chemical shift.

**Table 2 – NMR properties of biochars.**

| Sample                  | Aromaticity (%) |      | C <sub>obs</sub> (%) |     | −Δδ (ppm) |
|-------------------------|-----------------|------|----------------------|-----|-----------|
|                         | CP              | DP   | CP                   | DP  |           |
| <i>Wood</i>             |                 |      |                      |     |           |
| Oak 350                 | a               | a    | 51                   | 99  | 0.5       |
| Oak 450                 | 92.7            | 92.5 | 47                   | 101 | 1.3       |
| Pine 450                | 89.2            | 92.7 | 44                   | 97  | 1.3       |
| Pine 550                | 94.5            | 95.1 | 61                   | 107 | 2.2       |
| <i>Crop residues</i>    |                 |      |                      |     |           |
| Hazelnut 350            | 85.4            | 88.4 | 48                   | 101 | 0.6       |
| Hazelnut 450            | 88.4            | 92.8 | 47                   | 103 | 1.3       |
| Hazelnut 550            | 94.8            | 95.5 | 54                   | 100 | 1.7       |
| Corn 400                | 81.8            | 86   | 52                   | 113 | 0.7       |
| Corn 500                | 92.6            | 96.6 | 44                   | 93  | 1.4       |
| Corn 600                | a               | 94.3 | 33                   | 87  | 2.8       |
| Soy 500                 | 84.4            | 87.8 | 45                   | 91  | 0.2       |
| Switch 500              | 83.9            | 88.4 | 33                   | 49  | 0.9       |
| Bamboo 400              | 91.3            | 95   | 29                   | 60  | 1.5       |
| Bamboo 500              | 90.6            | 90.8 | 41                   | 77  | 1.4       |
| Bamboo 600              | a               | 94   | 8                    | 53  | 4.6       |
| <i>Manure feedstock</i> |                 |      |                      |     |           |
| Bull manure 400         | 86              | 90.1 | 39                   | 105 | 0.4       |
| Bull manure 500         | 93.6            | 95   | 46                   | 95  | 0.9       |
| Bull manure 600         | 95.7            | 94.6 | 32                   | 75  | 1.5       |
| Dairy manure 400        | 85.7            | 89.9 | 43                   | 98  | 0.7       |
| Dairy manure 600        | 95.4            | 99.2 | 51                   | 87  | 2.1       |
| <i>Organic waste</i>    |                 |      |                      |     |           |
| Food 400                | 79.7            | 80.7 | 40                   | 81  | −0.2      |
| Food 500                | 80.2            | 85.8 | 35                   | 81  | 0.2       |
| Food 600                | a               | 97.8 | 5                    | 97  | 1.5       |
| <i>Mill waste</i>       |                 |      |                      |     |           |
| Paper 400               | a               | a    | 39                   | 62  | 0.3       |
| Paper 500               | a               | a    | 34                   | 97  | 1.2       |
| Paper 600               | a               | a    | 28                   | 68  | 2.7       |

<sup>a</sup> No value given due to difficulties in integrating <sup>13</sup>C NMR spectra.

aromatic signal inevitable. Finally, the low NMR observability for some of the spectra means signal-to-noise ratios are low and this reduces the reliability of integration.

Under these circumstances, we can provide only an approximate measure of aromaticity for a subset of the biochars (Table 2). These values were determined by integrating the alkyl C region that is not compromised by SSBs (10–50 ppm) and subtracting this value from 100. Uncertainty in these integral values is likely to be small ( $\pm 2\%$ ), based on previous replicate analysis of char materials [14]. Clearly this measure of aromaticity is only appropriate for the biochars for which alkyl C is the only type of non-aromatic C detected. Therefore the paper 400 °C and oak 350 °C biochars are excluded because they contain peaks other than alkyl or aromatic C (i.e. carbonate and carbohydrate C). Also excluded are the CP spectra of the following biochars: food 600 °C, paper 500 °C, paper 600 °C and bamboo 600 °C, due to their poor signal-to-noise ratios.

Aromaticity determined from the CP spectra is generally slightly lower than for the corresponding DP spectra, confirming that aromatic C is detected with lower efficiency than non-aromatic C in CP spectra, as discussed above. Generally, at production temperatures above 400 °C, aromaticity is >80% (Table 2), and there is a consistent trend of increasing aromaticity with increasing temperature (Fig. 2). There is also

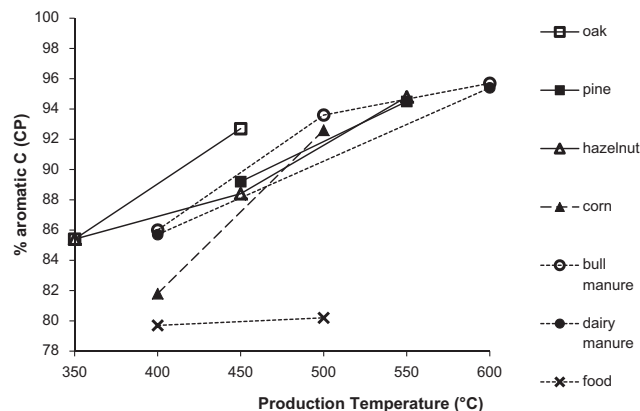


**Fig. 2 – Plot of aromaticity versus production temperature for biochars produced by slow pyrolysis at Best Energies Inc., USA (Enders et al., 2012).**

variation in aromaticity between feedstock types, indicating that feedstock also has a clear influence on the chemical structure of biochar (Fig. 2).

A second measure of biochar chemistry is the degree of aromatic condensation, which refers to the size and purity of the fused aromatic structures. The degree of aromatic condensation of the twenty-six biochars was determined using the novel “ring current” technique [17,23]. For larger and more pure (i.e. more condensed) aromatic structures,  $\Delta\delta$  becomes increasingly negative as the associated ring currents increase in strength. We showed in a previous study of a charcoal thermosequence that aromaticity was a quite insensitive measure of the changes in the chemical composition of char that occurred at temperatures >400 °C, whereas aromatic condensation was sensitive to the changes that occurred in the temperature range 400–1000 °C [17].

There is substantial variation in  $\Delta\delta$  values among the biochars (Fig. 3 and Table 2). Importantly, there are substantial differences in  $\Delta\delta$  values between biochars produced at the same temperature. However, within each series of biochars produced from the same feedstock,  $\Delta\delta$  decreases (becomes

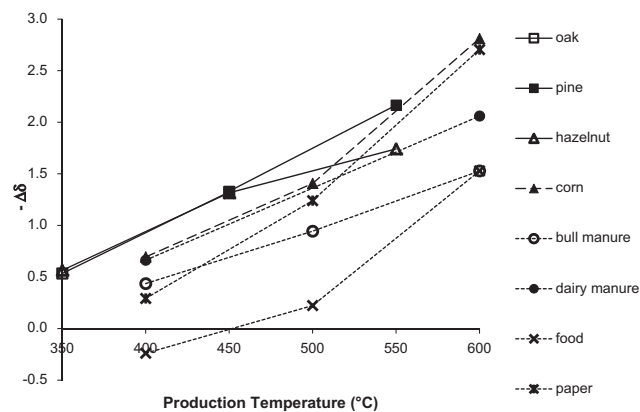


**Fig. 3 – Plot of  $-\Delta\delta$  versus production temperature for biochars produced by slow pyrolysis at Best Energies Inc., USA (Enders et al., 2012).**

more negative) monotonically and in most cases quite linearly (Fig. 3) with increasing production temperature. The exception to this is the biochars produced from grasses (cornstalks and bamboo), for which  $\Delta\delta$  values differ little between the biochars produced at 400 °C and 500 °C, but are much more negative for the biochars produced at 600 °C (Fig. 3).

#### 4. Discussion

The results of this study demonstrate that there is a clear relationship between production temperature and the chemical characteristics of aromaticity and aromatic condensation in biochar (Figs. 2 and 3). Regardless of what feedstock or pyrolysis process is used, as production temperatures increase, both aromaticity and the degree of aromatic condensation increase. This is due to the progressive dehydration, decarbonylation and decarboxylation reactions as the polycondensed aromatic structures are formed and polyaromatization reactions (i.e. growth in the size of aromatic sheets) become dominant [35,36]. The majority of these biochars (oak, pine, hazelnut, corn, bull manure, dairy manure, food and paper) were produced at the same pyrolysis plant and under the same pyrolysis conditions (Table 1, pyrolysis process b), other than production temperature. Thus, we can make direct comparisons of aromaticity and aromatic condensation values between feedstocks for these biochars.

Fig. 2 highlights the variation in aromaticity among biochars produced at the same temperature but from a different feedstock source. Woody feedstocks (oak and pine) tend to have the highest aromaticity. Oak has a greater aromaticity compared to pine which is more similar to that of the bull manure biochar, which may be due to the feedstock used to produce this biochar comprising of a mixture of manure and sawdust (wood shavings). This is followed closely by the hazelnut biochar. Of the mineral-rich feedstock biochars, corn and dairy manure have similar aromaticity and food biochar has the lowest aromaticity.

Similar trends are evident in the aromatic condensation of the biochars (Fig. 3). Oak and pine biochars have the greatest degree of aromatic condensation, with minimal differences between the hardwood (oak) and the softwood (pine). This is consistent with other studies that have compared hardwood and softwood biochars [15,24], which found the greatest variation in molecular structure at lower production temperatures (<300 °C); as production temperatures increased the biochars became more similar. Of the mineral-rich feedstock biochars, which include crop residues (corn) and waste products (bull manure, dairy manure, paper and food), corn biochars had the greatest degree of aromatic condensation, although it was still lower than that of the woody feedstocks. Hazelnut and dairy manure produced the next most condensed biochars, while paper, bull manure and food produced biochars with the lowest degree of aromatic condensation. As a consequence, food and paper biochars produced at the higher temperatures have  $\Delta\delta$  values similar to that of woody biochars produced at lower temperatures.

Pyrolysis process conditions also play a role in the molecular structure of biochars. The soy and switch grass biochars were produced using a different pyrolysis method (fast

pyrolysis). Compared with corn biochars (i.e. a biochar produced from a similar biomass) produced at a similar production temperature, they are less condensed. Similar findings have been reported in a previous comparison between biochars produced under slow and fast pyrolysis conditions [37]. This could be due to the shorter heat treatment time to that of the slow pyrolysis method. The bamboo biochars were produced using slow pyrolysis, but at a different pyrolysis plant (Table 1, pyrolysis process c) to that used for the majority of biochars (Table 1, pyrolysis process b). The bamboo 600 °C biochar had the greatest degree of aromatic condensation of all the biochars studied. This may reflect differences in heat treatment time between the two slow pyrolysis plants, but may also be due to differences in starting biomass. Unfortunately, we did not have biochars produced at the two plants from the same biomass.

Across the set of biochars in this study, aromaticity and aromatic condensation were strongly correlated ( $r^2 = 0.79$ ), and the relationship between these two parameters was quite linear (Fig. 4). This indicates that aromaticity and aromatic condensation, although essentially independent measures, co-vary for these biochars. As a result, both provide similar assessments of the carbonisation process of biochar. Since  $\Delta\delta$  is a less expensive and more rapid measurement to the traditional CP NMR experiment, we suggest it should be the method of choice.

The co-variation of aromaticity and aromatic condensation is in apparent contrast to our previous findings for a thermosequence of chars produced from one biomass (chestnut wood), for which we reported a rapid increase in aromaticity through a lower temperature range (200–400 °C), followed by a steady increase in aromatic condensation through a higher temperature range (400–1000 °C) [17]. However, it should be noted that the production temperatures of the biochars in this study span the region where both measures are reasonably sensitive. Inclusion of biochars produced at lower or higher temperatures would likely see this linear relationship break down as aromaticity condensation would not continue to decrease in the lower temperature range and aromaticity would not continue to increase in the higher temperature range. Biochars produced from some feedstocks show slightly

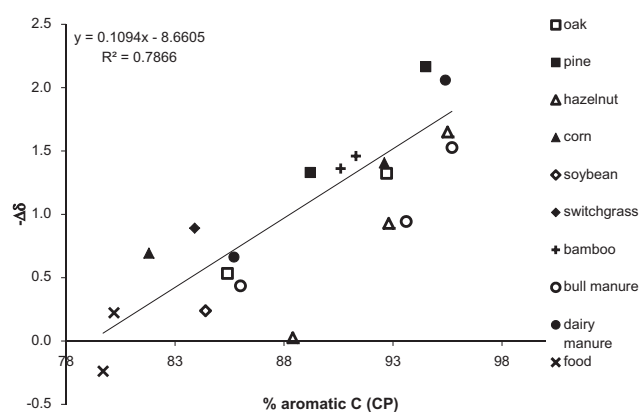


Fig. 4 – Plot of aromatic condensation ( $-\Delta\delta$ ) versus aromaticity for biochars produced from multiple feedstocks.

different relationships between aromaticity and aromatic condensation. For example, the bull manure feedstock produces biochars that have a low degree of condensation relative to their aromaticity (i.e. they appear below the line of best fit in Fig. 4). Conversely, corn, switch grass and pine biochars have a high degree of condensation relative to their aromaticity (i.e. appear above the line of best fit in Fig. 4). These observations suggest that the pathway by which these aromatic structures are formed may differ slightly depending upon not only production variables such as production temperature but also upon feedstock properties, which range from mineral-poor woody materials to mineral-rich manures and crop residues.

The relationship between  $\Delta\delta$  values and the mean residence time (MRT) established in a previous long-term incubation study [9] allows us to estimate the MRT for the biochars analysed in this study under the incubation conditions used by Singh et al. [9] (i.e. at room temperature in the absence of nutrient or moisture limitation but in a low organic matter, high clay soil). According to the relationship  $MRT = 148 \times e^{1.144 \times -\Delta\delta}$  [9], MRT is <260 years for biochars with  $-\Delta\delta$  values <0.5 (i.e. most of the biochars produced at the lowest temperatures of  $\leq 400^\circ\text{C}$ ), >460 years for biochars with  $-\Delta\delta$  values >1.0 (i.e. most of the biochars produced at intermediate temperatures of  $\sim 500^\circ\text{C}$ ), and >1400 years for biochars with  $-\Delta\delta$  values >2.0 (i.e. most of the biochars produced at the highest temperatures of  $\sim 600^\circ\text{C}$ ). Since the Singh et al. [9] study didn't include biochars with  $-\Delta\delta$  values >2.1, this formula cannot be used to estimate MRT for biochars with  $-\Delta\delta$  beyond this, other than to say they would likely be longer still. It should be kept in mind that MRT of biochar is likely to be strongly affected by environmental conditions. Nonetheless, these estimates indicate that (i) the biochars used in this study are likely to have MRTs of 100 years or more; and (ii) the MRT of biochars produced from different feedstocks and at different temperatures will vary by at least an order of magnitude. The significance of this last point is that the sequestration value of these different biochars varies considerably.

## 5. Conclusions

Our results demonstrate that two chemical properties, aromaticity and the condensation of these aromatic structures, are clearly influenced by production temperature and feedstock. Carbon-13 NMR spectra acquired using the CP and DP techniques were generally similar in appearance but aromaticity was slightly higher and observability much higher when determined using DP. Feedstocks with higher lignin contents, such as woody materials, were found to form more condensed aromatic structures and with a higher degree of aromaticity compared to biochars from mineral-rich feedstocks (e.g. crop residues) and waste materials (e.g. manures, food waste and paper mill waste) produced at the same production temperature. The composition of the feedstock thus plays an important role in the chemical composition of the biochar and this is likely to have follow-on effects in the performance of biochar as a soil amendment and as a carbon sink. There was a strong correlation between aromaticity and aromatic condensation, and given that measurement of

aromatic condensation is faster and also not affected by problems that compromise measurement of aromaticity (low and variable observability and overlap of aromatic spinning sidebands with the central bands of non-aromatic carbon types), we recommend measurement of aromatic condensation alone as a primary method for gauging organic structures in biochars.

## Acknowledgements

This project was supported by funding from the Australian Government under its Climate Change Research Program and by the Grains Research and Development Corporation.

## REFERENCES

- [1] Lehmann J, Joseph S. Biochar for environmental management: an introduction. In: Lehmann J, Joseph S, editors. *Biochar for environmental management*. London: Earthscan; 2009. p. 1.
- [2] Glaser B, Lehmann J, Zech W. Ameliorating physical and chemical properties of highly weathered soils in the tropics with charcoal – a review. *Biol Fertl Soils* 2002;35:219.
- [3] Bird MI, Moyo C, Veenendaal EM, Lloyd J, Frost P. Stability of elemental carbon in a savanna soil. *Global Biogeochem Cycles* 1999;13:923.
- [4] Hilscher A, Knicker H. Carbon and nitrogen degradation on molecular scale of grass-derived pyrogenic organic material during 28 months of incubation in soil. *Soil Biol Biochem* 2011;43:261.
- [5] Nguyen BT, Lehmann J, Kinyangi J, Smernik R, Riha SJ, Engelhard MH. Long-term black carbon dynamics in cultivated soil. *Biogeochemistry* 2008;89:295.
- [6] Keith A, Singh B, Singh BP. Interactive priming of biochar and labile organic matter mineralization in a smectite-rich soil. *Environ Sci Technol* 2011;45:9611.
- [7] Kuzyakov Y, Subbotina I, Chen H, Bogomolova I, Xu X. Black carbon decomposition and incorporation into soil microbial biomass estimated by  $^{14}\text{C}$  labeling. *Soil Biol Biochem* 2009;41:210.
- [8] Zimmerman AR. Abiotic and microbial oxidation of laboratory-produced black carbon (biochar). *Environ Sci Technol* 2010;44:1295.
- [9] Singh BP, Cowie AL, Smernik RJ. Biochar carbon stability in a clayey soil as a function of feedstock and pyrolysis temperature. *Environ Sci Technol* 2012;46:11770.
- [10] Preston CM, Schmidt MWI. Black (pyrogenic) carbon: a synthesis of current knowledge and uncertainties with special consideration of boreal regions. *Biogeosciences* 2006;3:397.
- [11] Krull ES, Baldock JA, Skjemstad JO, Smernik RJ. Characteristics of biochar: organo-chemical properties. In: Lehmann J, Joseph S, editors. *Biochar for environmental management, science and technology*. London: Earthscan; 2009. p. 53.
- [12] Hamer U, Marschner B, Brodowski S, Amelung W. Interactive priming of black carbon and glucose mineralisation. *Org Geochem* 2004;35:823.
- [13] Nguyen BT, Lehmann J. Black carbon decomposition under varying water regimes. *Org Geochem* 2009;40:846.
- [14] Baldock JA, Smernik RJ. Chemical composition and bioavailability of thermally, altered *Pinus resinosa* (red pine) wood. *Org Geochem* 2002;33:1093.

- [15] Ascough PL, Bird MI, Wormald P, Snape CE, Apperley D. Influence of production variables and starting material on charcoal stable isotopic and molecular characteristics. *Geochim Cosmochim Acta* 2008;72:6090.
- [16] Keiluweit M, Nico PS, Johnson M, Kleber M. Dynamic molecular structure of plant biomass-derived black carbon (biochar). *Environ Sci Technol* 2010;44:1247.
- [17] McBeath AV, Smernik RJ, Schneider MPW, Schmidt MWI, Plant EL. Determination of the aromaticity and the degree of aromatic condensation of a thermosequence of wood charcoal using NMR. *Org Geochem* 2011;42:1194.
- [18] Enders A, Hanley K, Whitman T, Joseph S, Lehmann J. Characterization of biochars to evaluate recalcitrance and agronomic performance. *Bioresour Technol* 2012;114:644.
- [19] Boateng AA, Daugaard DE, Goldberg NM, Hicks KB. Bench-scale fluidized-bed pyrolysis of switchgrass for bio-oil production. *Ind Eng Chem Res* 2007;46:1891.
- [20] Farrell M, Rangott G, Krull E. Difficulties in using soil-based methods to assess plant availability of potentially toxic elements in biochars and their feedstocks. *J Hazard Mater* 2013;250–251:29.
- [21] Smernik RJ, Oades JM. The use of spin counting for determining quantitation in solid state C-13 NMR spectra of natural organic matter 2. HF-treated soil fractions. *Geoderma* 2000;96:159.
- [22] Smernik RJ, Oades JM. The use of spin counting for determining quantitation in solid state <sup>13</sup>C NMR spectra of natural organic matter 1. Model systems and the effects of paramagnetic impurities. *Geoderma* 2000;96:101.
- [23] McBeath AV, Smernik RJ. Variation in the degree of aromatic condensation of chars. *Org Geochem* 2009;40:1161.
- [24] Czimczik CI, Preston CM, Schmidt MWI, Werner RA, Schulze ED. Effects of charring on mass, organic carbon, and stable carbon isotope composition of wood. *Org Geochem* 2002;33:1207.
- [25] David K, Pu YQ, Foston M, Muzzy J, Ragauskas A. Cross-polarization/magic angle spinning (CP/MAS) C-13 nuclear magnetic resonance (NMR) analysis of chars from alkaline-treated pyrolyzed softwood. *Energy Fuels* 2009;23:498.
- [26] Nguyen BT, Lehmann J, Hockaday WC, Joseph S, Masiello CA. Temperature sensitivity of black carbon decomposition and oxidation. *Environ Sci Technol* 2010;44:3324.
- [27] Pastorova I, Botto RE, Arisz PW, Boon JJ. Cellulose char structure – a combined analytical PY-GC-MS, FTIR, and NMR-study. *Carbohydr Res* 1994;262:27.
- [28] Knicker H, Hilscher A, Gonzalez-Vila FJ, Almendros G. A new conceptual model for the structural properties of char produced during vegetation fires. *Org Geochem* 2008;39:935.
- [29] Freitas JCC, Bonagamba TJ, Emmerich FG. C-13 High-resolution solid-state NMR study of peat carbonization. *Energy Fuels* 1999;13:53.
- [30] Preston CM. Carbon-13 solid-state NMR of soil organic matter – using the technique effectively. *Can J Soil Sci* 2001;81:255.
- [31] Emmerich FG, Rettori C, Luengo CA. ESR in heat treated carbons from the endocarp of babassu coconut. *Carbon* 1991;29:305.
- [32] Smernik RJ, Baldock JA, Oades JM. Impact of remote protonation on 13C CP/MAS NMR quantitation of charred and uncharred wood. *Solid State Nucl Magn Reson* 2002;22:71.
- [33] Smernik RJ, Baldock JA, Oades JM, Whittaker AK. Determination of T1ρH relaxation rates in charred and uncharred wood and consequences for NMR quantitation. *Solid State Nucl Magn Reson* 2002;22:50.
- [34] Freitas JCC, Passamani EC, Orlando MTD, Emmerich FG, Garcia F, Sampaio LC, et al. Effects of ferromagnetic inclusions on 13C MAS NMR spectra of heat-treated peat samples. *Energy Fuels* 2002;16:1068.
- [35] Bourke J, Manley-Harris M, Fushimi C, Dowaki K, Nunoura T, Antal MJ. Do all carbonized charcoals have the same chemical structure? 2. A model of the chemical structure of carbonized charcoal. *Ind Eng Chem Res* 2007;46:5954.
- [36] Nishimiya K. Analysis of chemical structure of wood charcoal by X-ray photoelectron spectroscopy. *J Wood Sci* 1998;44:56.
- [37] Brewer CE, Unger R, Schmidt-Rohr K, Brown RC. Criteria to select biochars for field studies based on biochar chemical properties. *Bioenergy Res* 2011;4:312.